

# Incorporation of monovalent cations into diopside to improve biomineralization and cytocompatibility

H. Rahmani, E. Salahinejad\*

Faculty of Materials Science and Engineering, K. N. Toosi University of Technology, Tehran, Iran

## ARTICLE INFO

### Keywords:

Calcination (A)  
Spectroscopy (B)  
Silicate (D)  
Biomedical applications (E)

## ABSTRACT

This paper aims to evaluate the structure, bioactivity, biodegradation and cytocompatibility of diopside ( $\text{CaMgSi}_2\text{O}_6$ ) doped with 2 mol% of Li, Na and K separately substituting for 1 mol% of Mg of diopside. An ethanolic, inorganic-salt coprecipitation method, followed by calcination at 900 °C, was used for synthesis. X-ray diffraction showed that the single-phase diopside structure is kept at this level of substitution; however, the crystallinity and lattice volume of diopside were changed depending on the size difference of the replacement components. According to in vitro biological studies, doping of all the alkali ions improves the bioactivity of diopside, with the highest and least effects obtained by K and Na, respectively. The MTT assay of osteoblast-like MG-63 cell cultures indicated that the cell viability and proliferation are improved as a result of using all the dopants, where the most enhancements were found for Na and K. It is eventually concluded that the incorporation of K into diopside ensures the optimal behaviors in terms of bioactivity and biocompatibility in vitro.

## 1. Introduction

Among bioactive/bioresorbable ceramics, magnesium-containing silicates in the both forms of crystalline and glass are under consideration in biomedicine [1,2]. Their typical benefit is higher mechanical strength in comparison to apatites and bioglass as the most prevalent bioactive/bioresorbable ceramics. One of the main members of this silicate group is diopside with the composition of  $\text{CaMgSi}_2\text{O}_6$ , i.e. a low level of calcium but the high amounts of magnesium and silicon. This particular ionic composition provides significant biocompatibility but limited bioactivity and biodegradation in comparison to the other members of magnesium-containing silicates.

Essentially, there are two approaches to enhancing the bioactivity of bioceramics: nanostructuring and using proper dopants. Pure nanocrystalline/nanoparticulate diopside has been synthesized by several wet-chemical methods like hydrothermal, sol-gel and coprecipitation [3–5]. In this regard, the application of chloride precursors has indicated several advantages, including lowering the formation temperature and the overall synthesis cost of single-phase diopside [6]. Regarding the doping approach, fluoride has been successfully used to control the apatite-formation ability of glassy and crystalline  $\text{CaMgSi}_2\text{O}_6$  (diopside) [7–9]. The presence of the alkali cations of  $\text{Li}^+$ ,  $\text{Na}^+$  and  $\text{K}^+$  in the body at trace contents creates the idea of their doping in diopside [10]. It would be worth mentioning that these

species have been previously employed in other bioceramics, leading to different and occasionally contradictory effects on biological behaviors [11–13].

In this work, with the aim of improving the bioactivity of diopside, Li, Na and K doping was originally conducted by a coprecipitation method using chloride precursors, followed by calcination. Afterwards, the obtained structure, bioactivity, biodegradation and cell viability were compared in vitro.

## 2. Experimental procedure

### 2.1. Sample preparation

Diopside ( $\text{CaMgSi}_2\text{O}_6$ ) was synthesized through a coprecipitation method using chloride precursors, ethanolic solution and ammonium precipitant, as detailed in Ref. [6]. Lithium (Li), sodium (Na) and potassium (K) was separately doped into diopside as follows. First,  $\text{CaCl}_2$ ,  $\text{MgCl}_2$ , and  $\text{LiCl}$  ( $\text{NaCl}$  or  $\text{KCl}$ ) at the molar ratio of 1:0.99:0.02 (i.e. 1 mol% of bivalent Mg was replaced with 2 mol% of the monovalent dopants for keeping the charge balance of the product) were added to ethanol under stirring. After complete dissolution,  $\text{SiCl}_4$  was added at 0 °C and stirred for 30 min. Finally, ammonium hydroxide solution was added to the solution for precipitation. The product was dried at 100 °C for 6 h, grounded and then calcined at 900 °C for 2 h.

\* Corresponding author.

E-mail address: [salahinejad@kntu.ac.ir](mailto:salahinejad@kntu.ac.ir) (E. Salahinejad).

<https://doi.org/10.1016/j.ceramint.2018.07.140>

Received 8 June 2018; Received in revised form 3 July 2018; Accepted 15 July 2018

0272-8842/ © 2018 Elsevier Ltd and Techna Group S.r.l. All rights reserved.

## 2.2. Structural characterization

X-ray diffraction (XRD, CuK $\alpha$  radiation), Fourier transform infrared spectroscopy (FTIR) and field emission scanning electron microscopy (FESEM) were utilized to study the phase, bonding and morphological characteristics of the calcined powders, respectively.

## 2.3. Bioactivity and biodegradation assessments

In order to compare the bioactivity of the synthesized samples *in vitro*, 0.1 gr of the powders was added to 40 ml of the simulated body fluid (SBF) and kept in an incubator at 36.5 °C for 7 and 14 days. The immersed samples, after washing and drying, were characterized by FESEM equipped with energy-dispersive X-ray spectroscopy (EDS) and Raman spectroscopy. The exposing SBFs were also analyzed by inductively coupled plasma optical emission spectroscopy (ICP-OES) and pH measurements.

## 2.4. Cell viability evaluation

For cellular studies, the powder samples were first sterilized in an ethanol solution, washed with phosphate-buffered saline, and then exposed to an UV radiation. Almost 20,000 osteoblast-like MG-63 cells were cultured on each sample for 24, 48 and 72 h. The assessment of the cell viability was performed by the MTT assay with three repetitions, in terms of the optical density of viable cells.

## 3. Results and discussion

### 3.1. Structural characterizations

Fig. 1 presents the XRD patterns of the calcined powder samples. Single-phase diopside structures (MgCaSi<sub>2</sub>O<sub>6</sub>) were identified in all of the undoped and doped samples by the PANalytical X'Pert HighScore software. Furthermore, the mean crystallite size of diopside was calculated by the Scherrer equation to be about 28.8, 28.5, 27.4 and 27.4 nm for the undoped, Li-doped, Na-doped and K-doped samples, respectively. The minor differences observed in the intensity of the associated XRD peaks in the different samples are related to the difference in the ionic radii and charges of the dopant and magnesium (substitution components). Indeed, the partial substitution of monovalent cations (dopants) for bivalent cations (Mg) breaks the network chains, as follows:



where D represents the monovalent dopants. This consequently gives rise to the reduction in crystallinity [14–18] and XRD peak intensities in comparison to the undoped powder. The contribution of the ionic

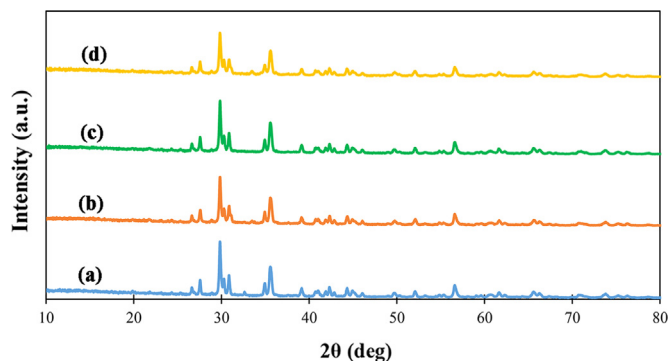


Fig. 1. XRD pattern of the undoped (a), Li- (b), Na- (c), and K- (d) doped samples after calcination. All of the diffraction peaks belong to diopside (Ref. Code: 00-017-0318).

**Table 1**  
Crystallographic data of diopside in the different doped structures.

Sample	a (Å)	b (Å)	c (Å)	$\beta$ (°)	V (Å <sup>3</sup> )
Undoped	9.759	8.933	5.265	105.91	441.341
Li-doped	9.752	8.929	5.267	105.98	440.903
Na-doped	9.756	8.933	5.266	105.88	441.391
K-doped	9.760	8.934	5.266	105.83	441.796

radius differences is described below in parallel with the network volume variations.

Diopside has a monoclinic structure with the lattice parameters of  $a \neq b \neq c$  and the axial angles  $\alpha = \gamma = 90 \neq \beta$ , where the network volume (V) is equal to “ $abc \sin \beta$ ”. The mentioned crystallographic data were extracted from the diffraction parameters of the most intense XRD peaks, as tabulated in Table 1. According to these results, compared to the undoped sample, the network volume for the sodium- and potassium-doped structures has increased, but it has decreased for the lithium-doped one. Doped ions are essentially located in the vacant lattice sites of the network which are pre-existing or created due to the partial removal of magnesium. As a result, doping distorts the network, depending on the charge and relative size of the substitution components. A larger dopant would distort the lattice, but the replacement of a dopant with an equal or smaller size would be easier. In this study, lithium ions are smaller, potassium ions are larger, and sodium ions are slightly larger (almost equal to) than magnesium ions. Lithium ions tend to react with oxygen existing in the network and to accommodate in the interstitial sites of the silicate network [19]. Nonetheless, sodium and potassium ions are substitutionally replaced with magnesium ions, where the lattice distortion generated by potassium is higher. These facts fairly explain the difference of the network volumes listed in Table 1. Typically, sodium with an ionic radius close to magnesium has led to the least distortion and thereby the closest lattice volume and XRD peak intensity to pure diopside.

Fig. 2 indicates the FTIR pattern of the synthesized samples after calcination. For all the samples, the peaks around 475 and 517  $\text{cm}^{-1}$  are attributed to the O-Mg-O group. Comparatively, these characteristic peaks display a reduced intensity after doping, as a result of the decrease in the concentration of magnesium which is partially replaced. The peaks of 635 and 675  $\text{cm}^{-1}$  belong to O-Si-O; in addition, vibrations at 865, 970 and 1080  $\text{cm}^{-1}$  are assigned to the symmetric stretching of Si-O [20]. An additional peak for the Li-doped sample at 1715  $\text{cm}^{-1}$  suggests the incorporation of Li ions [21]. Also, vibrations at around 2370  $\text{cm}^{-1}$  in the K- and Na-doped samples are attributed to the introduction of the related dopant in the structure [22,23].

Fig. 3 depicts the FESEM micrograph of the calcined powders. The pure diopside powder particles exhibit irregular shapes with a size of almost 80–800 nm. The Li-doped particles can be categorized into two

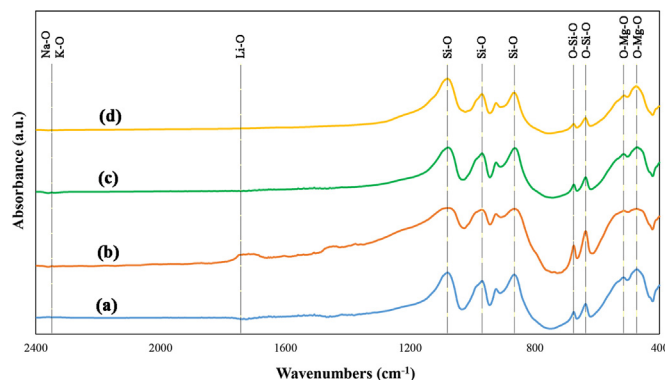


Fig. 2. FTIR spectra of the undoped (a), Li- (b), Na- (c), and K- (d) doped samples after calcination.

Download English Version:

<https://daneshyari.com/en/article/10155377>

Download Persian Version:

<https://daneshyari.com/article/10155377>

[Daneshyari.com](https://daneshyari.com)